



A 3D Human Lymphatic Vessel-on-Chip Reveals the Roles of Interstitial Flow and VEGF-A/C for Lymphatic Sprouting and Discontinuous Junction Formation

Isabelle S. Ilan^{1,2} · Aria R. Yslas¹ · Yansong Peng¹ · Renhao Lu¹ · Esak Lee^{1,3}

Received: 15 February 2023 / Accepted: 14 August 2023
© The Author(s) under exclusive licence to Biomedical Engineering Society 2023

Abstract

Introduction Lymphatic vessels (LVs) maintain fluid homeostasis by draining excess interstitial fluid, which is accomplished by two distinct LVs: initial LVs and collecting LVs. The interstitial fluid is first drained into the initial LVs through permeable “button-like” lymphatic endothelial cell (LEC) junctions. Next, the drained fluid (“lymph”) transports to lymph nodes through the collecting LVs with less permeable “zipper-like” junctions that minimize loss of lymph. Despite the significance of LEC junctions in lymphatic drainage and transport, it remains unclear how luminal or interstitial flow affects LEC junctions in vascular endothelial growth factors A and C (VEGF-A and VEGF-C) conditions. Moreover, it remains unclear how these flow and growth factor conditions impact lymphatic sprouting.

Methods We developed a 3D human lymphatic vessel-on-chip that can generate four different flow conditions (no flow, luminal flow, interstitial flow, both luminal and interstitial flow) to allow an engineered, rudimentary LV to experience those flows and respond to them in VEGF-A/C.

Results We examined LEC junction discontinuities, lymphatic sprouting, LEC junction thicknesses, and cell contractility-dependent vessel diameters in the four different flow conditions in VEGF-A/C. We discovered that interstitial flow in VEGF-C generates discontinuous LEC junctions that may be similar to the button-like junctions with no lymphatic sprouting. However, interstitial flow or both luminal and interstitial flow stimulated lymphatic sprouting in VEGF-A, maintaining zipper-like LEC junctions. LEC junction thickness and cell contractility-dependent vessel diameters were not changed by those conditions.

Conclusions In this study, we provide an engineered lymphatic vessel platform that can generate four different flow regimes and reveal the roles of interstitial flow and VEGF-A/C for lymphatic sprouting and discontinuous junction formation.

Keywords Lymphatic vessel-on-chip · Lymphatic junction · Luminal flow · Interstitial flow · Vascular endothelial growth factor C · Lymphatic sprouting

Abbreviations

BSA Bovine serum albumin
ECM Extracellular matrix

EGM-2MV Microvascular endothelial cell growth medium 2
FLT1 FMS-related receptor tyrosine kinase 1
JAM-A Junctional adhesion molecule-A
LECs Lymphatic endothelial cells
LVs Lymphatic vessels
LYVE-1 Lymphatic vessel endothelial hyaluronan receptor 1
NRP1 Neuropilin 1
PBS Phosphate buffered saline
PBST Phosphate buffered saline with Triton-X
PDMS Polydimethylsiloxane
Prox1 Prospero homeobox 1
VE-cadherin Vascular endothelial cadherin
VEGF-A Vascular endothelial growth factor A
VEGF-C Vascular endothelial growth factor C

Associate Editor Owen McCarty oversaw the review of this article.

✉ Esak Lee
el767@cornell.edu

¹ Nancy E. and Peter C. Meinig School of Biomedical Engineering, Cornell University, Ithaca, NY 14853, USA

² College of Human Ecology, Cornell University, Ithaca, NY 14853, USA

³ Nancy E. and Peter C. Meinig School of Biomedical Engineering, College of Engineering, Cornell University, 302 Weill Hall, 237 Tower Road, Ithaca, NY 14853, USA

VEGF-D	Vascular endothelial growth factor D
VEGFR2	Vascular endothelial growth factor receptor 2
VEGFR3	Vascular endothelial growth factor receptor 3
2D	Two-dimensional
3D	Three-dimensional

Introduction

The lymphatic system is a unidirectional conduit network in vertebrates, comprised of lymphatic vessels and lymphoid organs such as lymph nodes [1]. The lymphatic vasculature drains excess interstitial fluid that is leaked from blood capillaries and forms “lymph”, then transports the lymph to larger lymphatic vessels and lymph nodes, and ultimately returns the lymph to the blood circulation through the subclavian veins [2]. In addition to maintaining fluid homeostasis, the lymphatic system is necessary for transporting antigen-presenting cells and lymphocytes to lymph nodes to regulate antigen-specific adaptive immune responses [3]. Moreover, the lymphatic system plays a role in the absorption of dietary lipids in the small intestines and the removal of metabolic wastes in the brain [4, 5]. The lymphatic vasculature is further implicated in a range of diseases [6, 7]. Thus, failures in lymphatic drainage due to deficient, malformed, or dysfunctional lymphatic vessels are associated with lymphedema, lipedema, immune disorders, metabolic diseases, cancers, and neurodegenerative diseases [8–11].

Lymphatic drainage is accomplished by two anatomically distinct lymphatic vessels (LVs): initial LVs and collecting LVs. The interstitial fluid is first drained into the initial LVs, and then the drained fluid transports through the collecting LVs. Lymphatic drainage and transport are regulated by cell-cell junctions between lymphatic endothelial cells (LECs) in those vessels. In physiological conditions, these LEC junctions differ throughout the lymphatic vessel network between the initial LVs and the collecting LVs. The blind-ended initial LVs are a branched set of lymphatic capillaries necessary for the initial drainage of interstitial fluid [12]. To facilitate the interstitial fluid drainage, initial LVs lined with LECs that are oak leaf shaped with a discontinuous basal lamina and attached anchoring filaments, respond to the interstitial fluid flow and form permeable, button-like LEC junctions [12–15]. In contrast, collecting LVs are necessary for luminal lymph transport to the larger lymphatic vessels and lymph nodes. The collecting LVs respond to the luminal flow and form less permeable zipper-like LEC junctions to minimize the loss of lymph during the luminal transport. Moreover, collecting LVs are surrounded by lymphatic smooth muscle cells (LSMCs) and possess luminal valves (or secondary lymphatic valves) to allow lymphatic

contractile motions and prevent lymph backflow [15–17]. Elucidated through in vivo confocal microscopy using mouse models, discontinuous button-like LEC junctions that allow for interstitial fluid drainage were identified in initial LVs, and continuous, zipper-like LEC junctions were identified in collecting LVs that are less permeable and optimized for luminal fluid transport [12, 13]. However, despite the presence of specialized button-like and zipper-like LEC junctions in the initial and collecting LVs, where different flow patterns (interstitial flow and luminal flow) exist, the regulation of lymphatic junction morphogenesis under the interstitial flow and luminal flow is not well understood.

While there remain many components of button or zipper junction formation that need to be understood, a few factors have been identified that aid in the button or zipper junction plasticity in initial LVs [18]. During embryonic development, the junctions of the lymph sacs transform from zippers into buttons at E17.5 providing the mature initial LVs [13, 19]. In adult mice, as conducted with *Mycoplasma pulmonis*, there exists a transformation of buttons to zippers in the initial lymphatics in their lungs under infection [12, 18, 19]. Moreover, the transition can be reversed with the administration of dexamethasone, an anti-inflammatory agent, to return the initial lymphatics from the zippers to the buttons under the infectious condition [19]. Other studies have indicated that junction zippering is induced in lacteals (lymphatics in the small intestines), through vascular endothelial growth factor A (VEGF-A) and vascular endothelial growth factor receptor 2 (VEGFR2) signaling by deletion of neuropilin 1 (NRP1) and FMS-related receptor tyrosine kinase 1 (FLT1) in mice [13, 20], but opposingly, VEGFR2 inhibition enabled junction buttoning [20]. Another study has demonstrated that vascular endothelial growth factor C (VEGF-C) and vascular endothelial growth factor receptor 3 (VEGFR3) signaling is needed for promoting lymphatic junction buttoning [21]. Despite these previous findings, the roles of VEGF-A and VEGF-C in lymphatic junction formation under the luminal and interstitial flow are enigmatic.

Another essential component of lymphatic function is the process of lymphangiogenesis [22]. Lymphangiogenesis is the process in which new lymphatic vessels are generated from preexisting lymphatic vessels, which is a core process for embryonic development, lymphedema, and cancer metastasis [23]. A host of lymphangiogenic factors have been identified which can promote lymphatic sprouting, including VEGF-C and VEGF-D [24]. This system of lymphangiogenesis parallels the angiogenesis process in the blood vasculature which is driven by VEGF-A [25]. While these lymphangiogenic agents are known, there remain many components of the lymphangiogenic process that needs characterization; it remains unclear how varied lymphatic flow patterns, including both luminal and interstitial flow, influence lymphangiogenesis in VEGF-A/C conditions.

We acknowledge that animal models have been widely used to study LEC junctions and lymphatic sprouting. However, it is often difficult to isolate the relative contributions of biological factors such as VEGF-A/C signals as well as physical factors, such as luminal or interstitial fluid flow in animal models. By contrast, traditional cell cultures in two-dimensional (2D) dishes or transwells permit such identification, as they are highly controllable model systems, but they have not fully recapitulated the three-dimensional (3D) *in vivo* organization of these vasculatures [26–29]. Thus, there is a clear, unmet need for a 3D culture of human LECs. Based on that, there have been contributions from other groups and us to 3D *in vitro* models of lymphatic systems, which investigated lymphatic vessel (LV) sprouting [30–34], LV network formation [35–37], LV permeability [29, 38–40], lymph node formation [41–43], lymph valve morphogenesis [44–46], and LV interactions with cancer cells [47–51], and immune cells [52–54]. However, these previous *in vitro* models have not studied the roles of four flow patterns such as no flow, luminal flow, interstitial flow, and both luminal and interstitial flow in LEC junction formation and lymphatic sprouting in the presence of VEGF-A and VEGF-C.

In this study, we develop a unique 3D human lymphatic vessel-on-chip that can generate either luminal flow or interstitial flow, or both the luminal and interstitial flow to allow the engineered, rudimentary LV to experience those flow conditions and respond to the flows under the VEGF-A or VEGF-C stimulation. Utilizing the lymphatic vessel-on-chip system, we discovered that interstitial flow with VEGF-C cooperatively promotes discontinuous LEC junction formation that may be similar to the button junction formation, and interstitial flow with VEGF-A cooperatively promotes lymphatic sprouting, maintaining zipper-like and continuous LEC junctions.

Materials and Methods

Cell Culture

Primary human lymphatic endothelial cells (LECs), isolated from dermal tissues (foreskin) of newborn donors (male), were kindly gifted from Dr. Young Kwon Hong (University of Southern California). These LECs were previously characterized and validated by Dr. Hong's laboratory [34]. LECs were cultured in EGM-2MV media (Lonza, Switzerland) and maintained in standard tissue culture incubators at 37 °C, 95% humidity, and 5% CO₂. After LECs were introduced in the microfluidic devices, LEC media (EGM-2MV) was replaced with specialized VEGF-A media, VEGF-C media, or no VEGF media. For details, see section “[Microfluidics](#)”.

Microfluidics

The microfluidic device was created as we performed previously [40, 55–58]. Briefly, a silicon master was prepared to have two needle guides and a central oval-shaped extracellular matrix (ECM) space by utilizing a soft lithography method. The lymphatic vessel-on-chip was comprised of a polydimethylsiloxane (PDMS) gasket on top of the cover glass. In a 10:1 ratio, PDMS (Sylgard 184, Dow Chemical Company, Freeland, MI) was mixed with a curing agent, provided in the Sylgard PDMS kit. The mixture of PDMS and the curing agent were incubated overnight at 80 °C on the silicon master. After curing, the PDMS was removed from the silicon master and bonded to the cover glass through surface activation by plasma etching using PE-25 Plasma Cleaner (Plasma Etch Inc., Carson City, NV) with oxygen. For permanent bonding, the device was cured at 80 °C overnight finally providing the lymphatic vessel-on-chip devices (Fig. 1a, left). To allow hydrophilic surface modification, the device was plasma etched using PE-25 Plasma Cleaner with oxygen (Plasma Etch Inc., Carson City, NV). The device was treated with 0.01% poly-L-lysine (Sigma, St. Louis, MO) for 1 h, and rinsed with sterile water three times. Next, the device was treated with 1% glutaraldehyde (Electron Microscopy Sciences, Hartfield, PA) for 30 min, then rinsed with sterile water three times, and further rinsed in sterile water overnight at room temperature. Steel acupuncture needles with a diameter of 0.25 mm (Hawato, China) were sterilized with 70% ethanol and coated with bovine serum albumin (BSA, Sigma, St. Louis, MO). Two needles were inserted per device to make two hollow cylindrical channels (Fig. 1a, right). The device was dried using an air gun and sterilized with UV for 30 min. A collagen 1 gel (Corning, #356236, Corning, NY) was created with a final concentration of 2.5 mg/mL through buffering with phosphate-buffered saline (PBS) and titration with sodium hydroxide (NaOH, Sigma, St. Louis, MO) to a pH of 8.0. The collagen 1 was pipetted into the lymphatic vessel-on-chip devices and polymerized for 50 min at 37 °C. EGM-2MV media (Lonza, Switzerland) was added to the devices overnight. To create the channels in collagen 1, the two needles were removed from the devices. EGM-2MV media was added to the devices through the reservoirs and incubated overnight. The next day, primary human lymphatic endothelial cells (LECs) were resuspended at one million cells/mL in EGM-2MV media, and 100 µL of cell solution was added into one of the device channels through the connected reservoirs (Fig. 1a, right). For the first day after seeding, all of the devices received the same LEC media which was the EGM-2MV cell growth media. After the first day and for the remainder of the experiment, dependent on the group, the LEC media was the EGM-2MV cell growth medium modified by removing its growth factors and adding human recombinant VEGF-A (0.002 µg/mL,

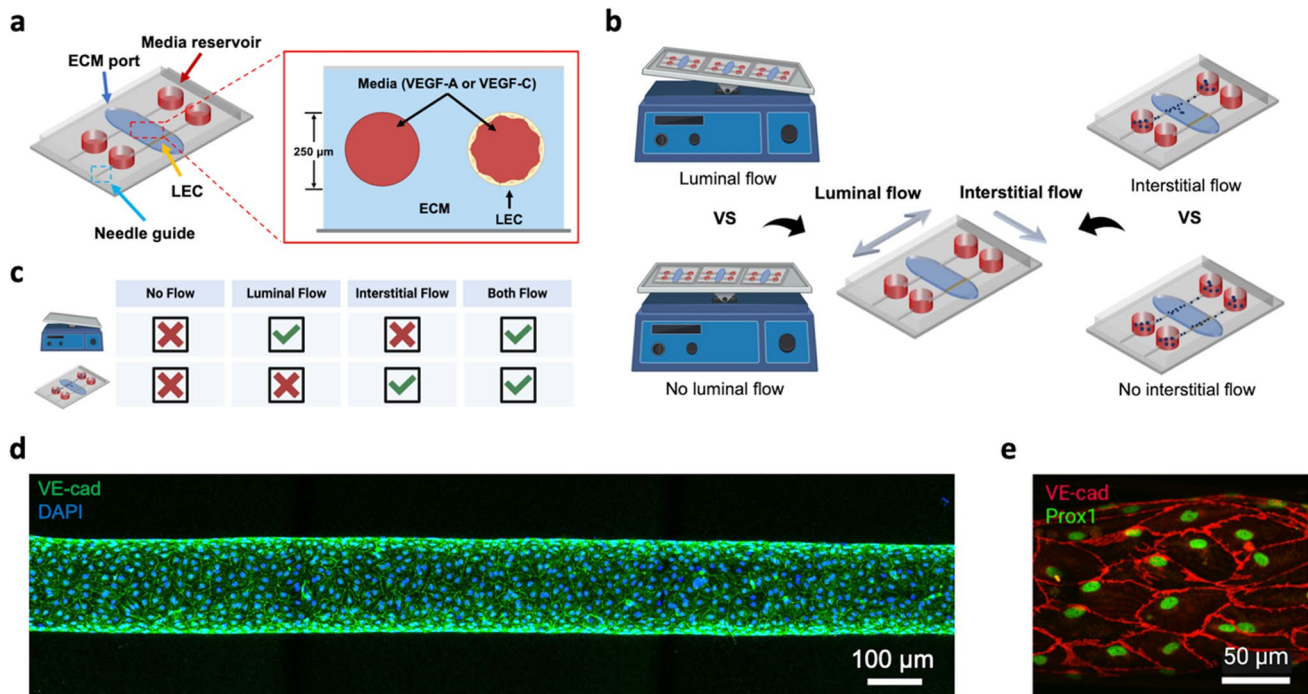


Fig. 1 An engineered 3D lymphatic vessel-on-chip model to investigate luminal and interstitial flow effects with VEGF-A or VEGF-C. **a** A schematic of an organotypic 3D lymphatic vessel model (lymphatic vessel-on-chip) with the human lymphatic endothelial cell (LEC) channel and the acellular channel within a 3D collagen matrix. Media with VEGF-A or VEGF-C was added into the four media reservoirs. **b** Methods to introduce luminal and interstitial flow. Left: a schematic of luminal flow, which involves leaving the device on a rocking platform with the same volume of media in all four reservoirs. Right: a schematic of interstitial flow, which requires a differential addition of media to the cellular and acellular channels, but no rocking. Black

dots represent the direction of interstitial flow (upper) or no interstitial flow (lower). **c** A schematic of four flow patterns: no flow, luminal flow, interstitial flow, and both flow. No flow does not involve rocking or differential media inputs, luminal flow requires rocking and no differential media inputs, interstitial flow requires no rocking but includes differential media inputs, and both flow requires rocking and differential media inputs. **d** A representative image of engineered lymphatic vessels with VE-cadherin staining (VE-cad: an adherens junction marker). **e** Prox1 staining of the engineered lymphatic vessels to show LEC identity (Prox1: a lymphatic endothelial marker)

PeproTech, Cranbury, NJ) or human recombinant VEGF-C (0.002 $\mu\text{g}/\text{mL}$, PeproTech, Cranbury, NJ). An additional third group was assessed that did not have any VEGF-A or VEGF-C. The devices were incubated for 2 days on a rocking platform in the tissue incubator to make sure the LECs were well adhered to the collagen channel, creating an engineered LV. Media was changed daily. After the second day of incubating on the rocking platform, specific flow patterns were instituted: (i) no flow, (ii) luminal flow, (iii) interstitial flow, and (iv) both luminal and interstitial flow as described below (Fig. 1b).

Induction of Differential Fluid Flows

We inducted four different flow patterns: no flow, luminal flow, interstitial flow, and both luminal and interstitial flow in our devices (Fig. 1b). The no flow group was created by filling all four reservoirs with the same amount of growth medium (200 μL in every reservoir) and putting the device on a flat and static surface in a regular tissue

culture incubator. The luminal flow group was created by filling all four reservoirs with the same amount of growth medium (200 μL in every reservoir) and leaving the device on a rocking platform, with the device channels parallel to the lateral edges of the platform in a regular tissue culture incubator. This allowed fluid to continuously flow through the lumen of the LEC channel. The rocker tilts the chips from -37° to $+37^\circ$ at a frequency of 2–3 rpm. The diameter of the microchannel is 0.25 mm. These conditions create approximately a shear stress of 3.5–4.5 dyne/cm^2 (Fig. 1b, left) [40]. This value is within the range of 4–12 dyne/cm^2 , which was determined as the *in vivo* value for rat mesenteric lymphatics [59]. In addition, according to the Hagen–Poiseuille equation, the velocity of luminal flow, is approximately 5.7–5.8 mm/s in our devices. This is physiologically relevant given that in rat mesenteric lymphatics, contraction propagates flow along the wall at a rate of 4–8 mm/s *in vivo* [60]. More detailed processes for obtaining these values for luminal flow are described in the Supplementary Information (Supplementary Materials and Methods).

The interstitial flow group was created by adding a differential amount of fluid to either side of the media reservoir (20 μL in each media reservoir of the LEC channel, and 200 μL in each media reservoir of the acellular channel), then the interstitial flow chips were maintained in the incubator on a flat/static surface. Differential amounts of fluid generate different heights of the fluid in the reservoirs, which results in differential hydrostatic fluid pressure between the two channels. As a result of the hydrostatic fluid pressure difference, created by the differential height of fluid in the reservoirs, the fluid seeks to equilibrate hydrostatic pressure by convecting across the 3D collagen from the acellular channel to the LEC channel. This convection induces interstitial fluid flow toward the LEC channel with a maximum flow rate of 1 $\mu\text{m/s}$ based on the distance between the two channels (7 mm) and the height difference of the fluid column between the two media reservoirs (7 mm). This flow rate is physiologically relevant, given the physiological range of interstitial flow rate in healthy tissues (0.0–1.0 $\mu\text{m/s}$) [61, 62]. To maintain a certain level of interstitial fluid pressure, a differential volume of media was added twice daily (Fig. 1b, right).

The both flow (luminal and interstitial flow) group was provided by combining our luminal and interstitial flow conditions. Briefly, both the luminal and interstitial flow group was maintained on the rocker, as per the luminal group's procedure, and a differential volume of media was added twice daily, as per the interstitial group's procedure. Each device was nourished with its specific media type (VEGF-A, VEGF-C, and no VEGF media) and maintained at its specific flow pattern for 4 days. The flow settings are summarized in Fig. 1c.

Immunostaining and Imaging in Microfluidics

The lymphatic vessel-on-chip devices were fixed with 4% paraformaldehyde (Electron Microscopy Sciences, Hartfield, PA) for 1 h at room temperature. The chips were treated with PBST (0.3% Triton-X, Sigma, St. Louis, MO in PBS) for 45 min at room temperature to permeate the cells in the device. The fixed and permeated devices were blocked with 3% BSA in PBS overnight at 4 °C. Primary antibodies detecting VE-cadherin (Abcam, UK, ab33168, 1:100), JAM-A (Santa Cruz Biotechnology, Dallas, TX, sc-53624, 1:100), and Prox1 (Abcam, UK, ab101851, 1:100) were incubated in a blocking buffer overnight at 4 °C. Primary antibodies were washed overnight in PBS at 4 °C. Secondary antibodies (all from Invitrogen, Carlsbad, CA, 1:500), Phalloidin (Life Technologies, Carlsbad, CA, 1:200), and DAPI (Sigma, St. Louis, MO, 1:500) were subsequently incubated in a blocking buffer overnight at 4 °C in dark. The secondary antibodies, phalloidin, and DAPI were washed overnight in PBS at 4 °C in dark. Images were acquired through confocal microscopy, utilizing the SP8 confocal microscope (Leica,

Germany) with a 10 \times and 40 \times objective. The images were z-stacked and adjusted for brightness and contrast using ImageJ [63]. To quantify junction discontinuities, two individuals, blinded, counted the number of discontinuities in the cell border of 15–30 randomly selected cells per vessel. The average values of one individual's quantifications were normalized to the average of the other individual's values to ensure that the range of discontinuities found was similar. Lymphatic sprouting was assessed by the quantification of the number of individual cells forming sprouts (based on DAPI and VE-cadherin expression) found beyond the lymphatic vessel wall in the collagen matrix. The thickness of the junctions was assessed with ImageJ by measuring the thickness of the cell borders at 4 spaced-out points per cell to create an average thickness measurement per cell [63]. 15–30 cells were selected per vessel in assessing the junction thickness and two individuals similarly assessed and compiled their data in a blinded manner. ImageJ was utilized to assess lymphatic vessel diameter on the 10 \times images [63].

Statistics

Data analyses were performed by two individuals in a blinded manner throughout the study. Independent two-sample populations were assessed utilizing an unpaired, two-sample *t*-test with a normal distribution assumption. When there were eight or more groups (including the two subcategories of media type and flow type), a two-way ANOVA was performed with a Tukey's HSD test, and when there were four groups (flow type comparison), a one-way ANOVA was performed with a Tukey's HSD test. $p < 0.05$ was the threshold for statistical significance. The *p*-values and sample numbers (biological replicates, *n*) are detailed in the figure legends. Data on the graphs represent average values, and all single data points were also presented in every plot. Error bars depict the Standard Error of the Mean (S.E.M.).

Results

LECs in Luminal or Interstitial Flow in VEGF-A or VEGF-C Generate and Maintain Engineered Lymphatic Vessels

To assess how engineered lymphatic vessels (LVs) respond to varying flow patterns under VEGF-A or VEGF-C conditions, we developed a lymphatic vessel-on-chip model that consists of two parallel microchannels, embedded in a 3D collagen 1 matrix and connected to media reservoirs (Fig. 1a, left). Human dermal microvascular lymphatic endothelial cells (LECs) were seeded into one channel to reconstitute a rudimentary, engineered LV (Fig. 1a, right).

The devices were divided into three media groups: VEGF-A, VEGF-C, and no VEGF (without VEGF-A or VEGF-C). VEGF-A or VEGF-C were introduced into our growth factor-depleted EGM-2MV media that was incorporated into the devices. Next, the VEGF-A, VEGF-C, and no VEGF groups were subdivided into four different groups with distinct flow patterns: (i) no flow, (ii) luminal flow, (iii) interstitial flow, and (iv) luminal and interstitial flow (“both flow”) (Fig. 1c). As described in the “Materials and Methods” section, the no flow group was maintained by providing equal volumes of media to the media reservoirs on a static surface. The luminal flow group was maintained by providing equal volumes of media to the media reservoirs on a rocking platform, which allows only a gravity-mediated luminal flow within the lymphatic channel. The interstitial flow group was prepared by applying differential volumes of fluid to the media reservoirs on a static surface, which allows only a hydrostatic pressure-mediated interstitial flow from the acellular channel to the lymphatic channel. Lastly, the both luminal and interstitial flow group was maintained by applying differential media volumes to the reservoirs (interstitial flow) and keeping the devices on a rocker (luminal flow) (Fig. 1b, c). As such, there were 12 experimental groups: VEGF-A/No Flow, VEGF-A/Luminal Flow, VEGF-A/Interstitial Flow, VEGF-A/Both Flow, VEGF-C/No Flow, VEGF-C/Luminal Flow, VEGF-C/Interstitial Flow, VEGF-C/Both Flow, No VEGF/No Flow, No VEGF/Luminal Flow, No VEGF/Interstitial Flow, and No VEGF/Both Flow.

In our 3D culture, we found that LECs in luminal or interstitial flow in VEGF-A or VEGF-C generate and maintain engineered lymphatic vessels (Fig. 1d). LECs in one of the representative devices expressed VE-cadherin, a vascular endothelial adherens junction marker in their junction areas (Fig. 1d). We further stained the engineered LVs with anti-Prox1 antibodies and confirmed the lymphatic endothelial identity in the cells we seeded and cultured in our devices (Fig. 1e). However, in the groups without VEGF-A or VEGF-C (no VEGF groups), engineered LVs with lumens were only maintained in the luminal flow and both flow groups (Supplementary Fig. 1). Surprisingly, in no VEGF conditions, interstitial flow and no flow were unable to form a lymphatic vessel with a lumen (Supplementary Fig. 1e). As such, data for this paper is represented based on the eight groups with either VEGF-A and VEGF-C, and the minimal acquired data for no VEGF is found in Supplemental Fig. 1a–d. The lack of vessel formation in the no VEGF groups in interstitial flow and no flow suggests the important role of having either consistent luminal flow or VEGF for the generation and maintenance of rudimentary LVs. Taken together, LECs in luminal and/or interstitial flow in VEGF-A or VEGF-C generate and maintain engineered lymphatic vessels, but no VEGF condition only allows vessel formation

when the luminal flow is involved, whether the luminal flow is alone or in conjunction with the interstitial flow.

Combining VEGF-C and Interstitial Flow Increases LEC Junction Discontinuity

Based on the device we created in Fig. 1, we examined the discontinuity of lymphatic endothelial cell (LEC) junctions as they varied between flow type and media type (Fig. 2). To assess LEC junction discontinuities, cells stained for VE-cadherin were imaged and adjusted on a threshold determined by Otsu’s method [64], and the number of junction discontinuities per cell was counted. Two individuals, in a blinded manner, separately quantified the number of discontinuities in the borders of 15–30 randomly selected cells within each vessel. The average values of one individual’s quantifications were normalized to the average of the other individual’s values to ensure that the range of discontinuities found was similar. This study had 4–6 biological replicates (the number of distinct devices/vessels) per group. To test whether the VE-cadherin signal is not a staining artifact but a valid signal, we co-stained the vessels with a tight junction marker, anti-JAM-A antibodies (JAM-A: Junctional adhesion molecule-A), and confirmed tight junction (JAM-A) colocalization with adherens junction (VE-cadherin) in the devices (Supplementary Fig. 2). Upon this confirmation, we quantified LEC junctions using the VE-cadherin staining images throughout the study.

We first combined all the data in VEGF-A or VEGF-C, regardless of their flow types to evaluate the roles of VEGF-A and VEGF-C in LEC junction formation (Fig. 2a). In general, VEGF-C appeared to loosen the cell junctions with significantly more discontinuities than VEGF-A ($p=0.0176$) (Fig. 2a). Next, we combined all of our data in each flow type, regardless of their growth factor conditions to assess the roles of flow in LEC junction formation (Fig. 2b). Using the one-way ANOVA with Tukey’s HSD test-based quantification of the discontinuities across flow types indicated no significant differences between any of the flow types when comparing flow irrespective of growth factors (Fig. 2b). The greatest difference, although not significant, between the flow types exists between luminal flow with the lowest discontinuities and interstitial flow with the highest discontinuities (Luminal Flow: 1.3 ± 0.1 ; Interstitial Flow: 1.87 ± 0.3 ; $p=0.15$).

When flow type and media type were analyzed together, VEGF-C in the interstitial condition appeared to loosen LEC junctions dramatically, as there were more junction discontinuities than LEC junction discontinuities in the other conditions (Fig. 2c). Using the two-way ANOVA with Tukey’s HSD test-based quantification of the discontinuities, we revealed that the effects of interstitial flow in VEGF-C become more pronounced, having more discontinuous

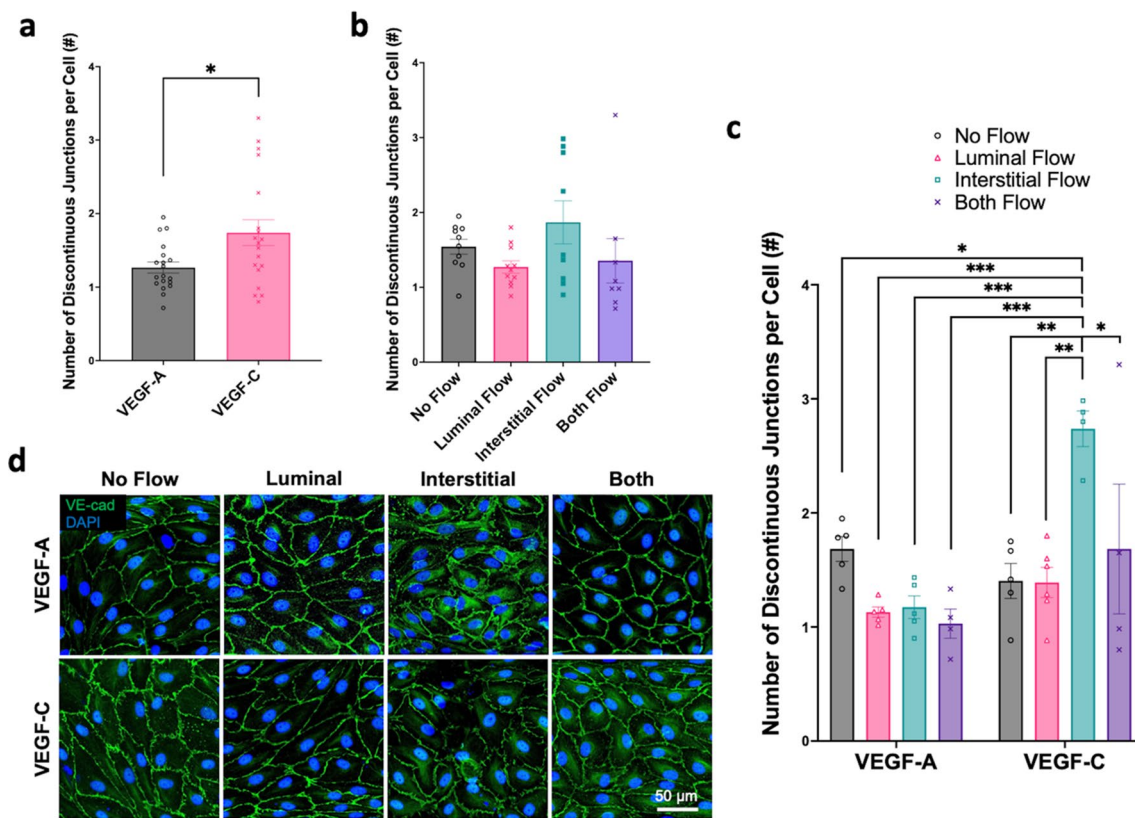


Fig. 2 LEC junction discontinuity with VEGF-A or VEGF-C and with different flow patterns. **a** Quantification of junction discontinuities per lymphatic endothelial cell (LEC) with VEGF-C or VEGF-A media. An unpaired Student t-test was used ($*p < 0.05$) with biological replicates (VEGF-A: $n = 19$; VEGF-C: $n = 19$; n represents whole vessels/devices). **b** Quantification of junction discontinuities per LEC between no flow, luminal flow, interstitial flow, and both flows. One-way ANOVA with Tukey's HSD tests was used with biological replicates (No Flow: $n = 10$; Luminal Flow: $n = 11$; Interstitial Flow: $n = 9$; Both Flow: $n = 8$). There was no significance between these

junctions than any other groups. The p-values of these comparisons were VEGF-A/No Flow vs. VEGF-C/Interstitial Flow, $p = 0.02$; VEGF-A/Luminal Flow vs. VEGF-C/Interstitial Flow, $p = 0.0002$; VEGF-A/Interstitial Flow vs. VEGF-C/Interstitial Flow, $p = 0.0003$; VEGF-A/Both Flow vs. VEGF-C/Interstitial Flow, $p = 0.0001$; VEGF-C/No Flow vs. VEGF-C/Interstitial Flow, $p = 0.0021$; VEGF-C/Luminal Flow vs. VEGF-C/Interstitial Flow, $p = 0.0011$; VEGF-C/Interstitial Flow vs. VEGF-C/Both Flow, $p = 0.0374$ (Fig. 2c). The representative VE-cadherin-stained images were shown in Fig. 2d. In the VEGF-A condition, more robust and continuous junctions were observed in all flow groups compared to the no flow group (Fig. 2d, upper). In the VEGF-C condition, there appear to be very few zipper junctions in the interstitial flow group as the discontinuities increase, however, luminal and both flow groups formed more zipper-like junctions with fewer discontinuities (Fig. 2d, lower). Taken together, VEGF-C independently

four groups. **c** Quantification of junction discontinuities per LEC between flow patterns and VEGF-C and VEGF-A media. Two-way ANOVA with Tukey's HSD tests was used ($*p < 0.05$, $**p < 0.01$, $***p < 0.001$) with biological replicates ($n = 4-6$; n represents whole vessels/devices). **d** Representative confocal images of engineered lymphatic vessels across flow patterns with VEGF-C or VEGF-A with anti-VE-cadherin antibody staining to show LEC adherens junctions and DAPI to show LEC nucleus. **a-c** Data are expressed as mean \pm S.E.M. and individual data are presented in the graphs

appeared to loosen junctions, and interstitial flow with VEGF-C induced greater discontinuities in LEC junctions.

VEGF-A in Interstitial Flow Alone or Both Interstitial and Luminal Flows Stimulates Lymphatic Sprouting with Maintaining Zipper-Like LEC Junctions

To assess the lymphangiogenic potential of different flow regimes with different media conditions, lymphatic sprouting was assessed in the lymphatic vessel-on-chip model (Fig. 3). Lymphatic sprouting was quantified by counting the number of matrix-invaded LECs forming lymphatic sprouts that had clear co-staining by DAPI and anti-VE-cadherin antibodies. Using the two-way ANOVA with Tukey's HSD test-based quantification, we found that under the VEGF-A condition, interstitial flow and both flow groups (interstitial flow and luminal flow) produced significantly more sprouts than luminal flow or no flow groups (Fig. 3a). VEGF-A/

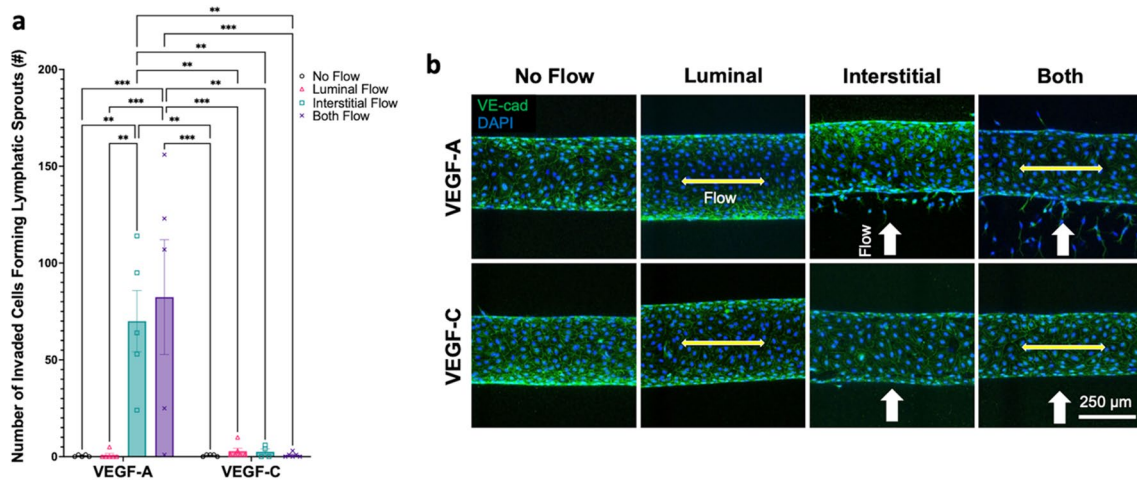


Fig. 3 Lymphatic sprouting with VEGF-A or VEGF-C and with different flow patterns. **a** Quantification of lymphatic sprouting between flow patterns and VEGF-C and VEGF-A media. Two-way ANOVA with Tukey's HSD tests was used (** $p < 0.01$, *** $p < 0.001$) with biological replicates ($n = 4-6$, n represents whole vessels/device). Data are expressed as mean \pm S.E.M. and individual data are presented in the graphs. **b** Representative confocal images of engineered lymphatic vessels across flow patterns with VEGF-C or VEGF-A with anti-VE-cadherin antibodies to show LEC adherens junctions and DAPI to show LEC nucleus. Double-headed, yellow arrows parallel to a vessel represent luminal flow, and single-headed white arrows perpendicular to a vessel represent interstitial flow (interstitial flow direction is from bottom to top in the image)

Interstitial Flow group had an average of 70 ± 15.8 sprouts per vessel and VEGF-A/Both Flow group had an average of 82.4 ± 29.7 sprouts. The other groups, including VEGF-A/Luminal Flow, VEGF-A/No Flow, and VEGF-C with all types of flow had consistently low values of sprouting between 0 and 5 sprouts per vessel, with one outlier of one data point with 10 sprouts in VEGF-C/Luminal flow group. Overall, VEGF-A with the interstitial flow or both interstitial and luminal flows had significantly more sprouting compared to every other group as shown in these p-values: VEGF-A/No Flow vs. VEGF-A/Interstitial Flow, $p = 0.0035$; VEGF-A/No Flow vs. VEGF-A/Both Flow, $p = 0.0004$; VEGF-A/Luminal Flow vs. VEGF-A/Interstitial Flow, $p = 0.0022$; VEGF-A/Luminal Flow vs. VEGF-A/Both Flow, $p = 0.0002$; VEGF-A/Interstitial Flow vs. VEGF-C/No Flow, $p = 0.0036$; VEGF-A/Interstitial Flow vs. VEGF-C/Luminal Flow, $p = 0.0031$; VEGF-A/Interstitial Flow vs. VEGF-C/Interstitial Flow, $p = 0.0093$; VEGF-A/Interstitial Flow vs. VEGF-C/Both Flow, $p = 0.0022$; VEGF-A/Both Flow vs. VEGF-C/No Flow, $p = 0.0004$; VEGF-A/Both Flow vs. VEGF-C/Luminal Flow, $p = 0.0003$; VEGF-A/Both Flow vs. VEGF-C/Interstitial Flow, $p = 0.0013$; VEGF-A/Both Flow vs. VEGF-C/Both Flow, $p = 0.0002$ (Fig. 3a). The representative VE-cadherin and DAPI staining for the sprouting images show clearly increased numbers of lymphatic sprouting in VEGF-A, toward the interstitial fluid pressure gradient (in other words, against the direction of the interstitial flow, white arrows) when the interstitial flow is involved, whether the interstitial flow is alone or in conjunction with the luminal flow (Fig. 3b). Interestingly, these VEGF-A

based sprouting conditions did not form discontinuous LEC junctions in our junction discontinuity analyses (Fig. 2c, d). Taken together, VEGF-A in interstitial flow or both flow conditions stimulates lymphatic sprouting but still maintains continuous, zipper-like LEC junctions.

VEGF-A/VEGF-C and Varied Flow Patterns Do Not Change LEC Junction Thickness and Lymphatic Vessel Diameters

Next, to further assess vessel characteristics as they modulate in varying flow and media conditions, LEC junction thickness and lymphatic vessel diameters were determined in the lymphatic vessel-on-chip model (Figs. 4, 5). LEC junction thickness was assessed in a blinded manner by two individuals by measuring LEC junction widths at four points per cell for 15–30 cells per vessel utilizing ImageJ software [63]. The average values of the two individuals were compiled and we had 5–6 biological replicates (vessels/devices) per group. Like our junction discontinuity data, we combined all of the data in VEGF-A or VEGF-C, regardless of their flow types to assess the roles of growth factors in junction thickness. There were no significant differences found between the thickness of the LEC junctions between the two growth factor cohorts (Fig. 4a). Next, we combined all of the data in each flow type, regardless of the types of growth factors to examine the roles of flows in junction thickness. When comparing the four flow patterns, there were no significant differences between the four groups (Fig. 4b). Lastly, when assessing the data with both media types and flow types

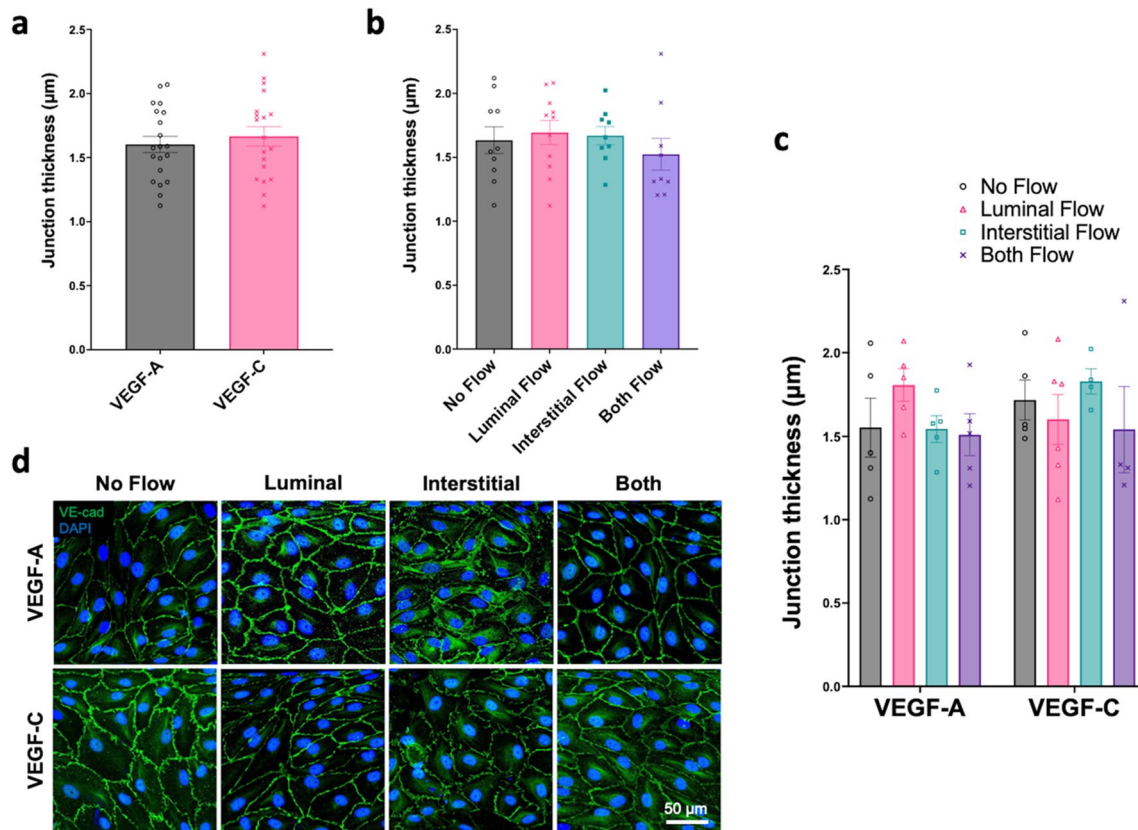


Fig. 4 LEC junction thickness with VEGF-A or VEGF-C and with different flow patterns. **a** Quantification of LEC junction thickness with VEGF-C or VEGF-A media. Unpaired Student t-test was used with biological replicates (VEGF-A: $n=20$; VEGF-C: $n=19$; n represents whole vessels/devices). All comparisons showed no significance. **b** Quantification of LEC junction thickness between no flow, luminal flow, interstitial flow, and both flow. One-way ANOVA with Tukey's HSD tests was used with biological replicates (No Flow: $n=10$; Luminal Flow: $n=11$; Interstitial Flow: $n=9$; Both Flow: $n=9$). All comparisons showed no significance. **c** Quantification

of LEC junction thickness between flow patterns and VEGF-C and VEGF-A media. Two-way ANOVA with Tukey's HSD tests was used with biological replicates ($n=4-6$; n represents whole vessels/devices). All comparisons showed no significance. **d** Representative confocal images of engineered lymphatic vessels across flow patterns with VEGF-C or VEGF-A with anti-VE-cadherin antibody staining to show LEC adherens junctions and DAPI to show LEC nucleus. **a-c** Data are expressed as mean \pm S.E.M. and individual data are presented in the graphs

combined, there were again no significant differences in the thickness of the junctions (Fig. 4c). The representative VE-cadherin staining for assessing junction thickness images were shown in Fig. 4d.

To assess LEC contractility under different flow and growth factor conditions, the diameter of engineered lymphatic vessels was assessed across flow types and media types (Fig. 5). In general, more contractile LECs form a lymphatic vessel with a smaller diameter, or less contractile LECs form a lymphatic vessel with a bigger diameter. When we combined all of our data in VEGF-A or VEGF-C, regardless of the flow regimes, there were no significant differences in lymphatic vessel diameters (Fig. 5a). Additionally, there was no difference in diameters when we combined all of our data in different flow conditions, regardless of the growth factors used (Fig. 5b). Lastly, the four flow patterns did not institute significantly different diameters from each

other either in VEGF-A and VEGF-C (Fig. 5c). The representative vessel images were shown in Figure 5d. Taken together, VEGF-A, VEGF-C, and varied flow patterns do not significantly influence LEC junction thicknesses and LEC contractility-related lymph vessel diameters in our lymphatic vessel-on-a-chip model.

Discussion

In this study, we engineered an in vitro, 3D human lymphatic vessel-on-chip model to study lymphatic endothelial cell (LEC) junction morphogenesis and lymphatic sprouting under luminal and interstitial flow conditions with VEGF-A and VEGF-C treatment (Fig. 1). We instituted four distinct fluid flow patterns in our devices: (i) no flow, (ii) luminal flow, (iii) interstitial flow, (iv) luminal and interstitial flow

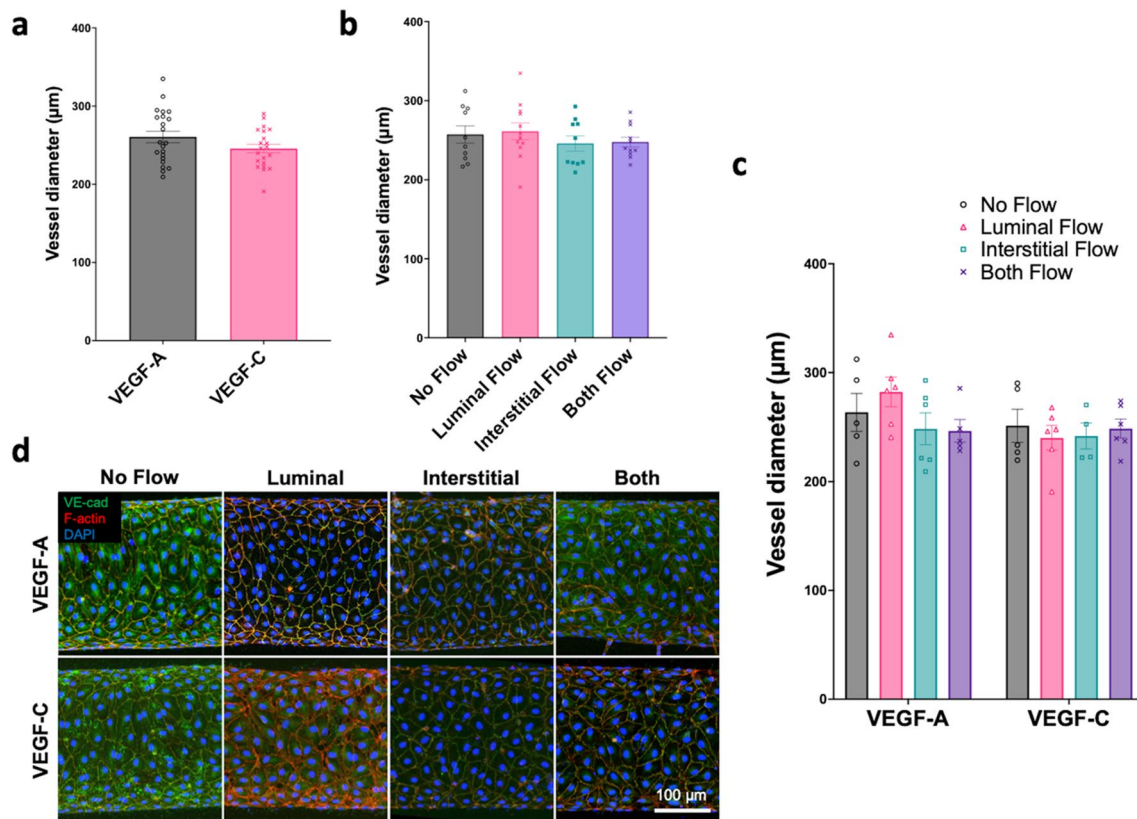


Fig. 5 Lymphatic vessel diameter with VEGF-A or VEGF-C and with different flow patterns. **a** Quantification of lymphatic vessel diameter with VEGF-C or VEGF-A media. Unpaired Student t-test was used with biological replicates (VEGF-A: $n=22$; VEGF-C: $n=21$; n represents whole vessels/devices). All comparisons showed no significance. **b** Quantification of lymphatic vessel diameter between no flow, luminal flow, interstitial flow, and both flow. One-way ANOVA with Tukey's HSD tests was used with biological replicates (No Flow: $n=10$; Luminal Flow: $n=12$; Interstitial Flow:

$n=10$; Both Flow: $n=11$). All comparisons showed no significance. **c** Quantification of lymphatic vessel diameter between flow patterns and VEGF-C and VEGF-A media. In two-way ANOVA with Tukey's HSD tests ($n=4-6$; n represents whole vessels/devices). All comparisons showed no significance. **d** Representative confocal images of engineered lymphatic vessels across flow patterns with VEGF-C or VEGF-A with anti-VE-cadherin antibodies, phalloidin (F-actin), and DAPI staining. **a-c** Data are expressed as mean \pm S.E.M. and individual data are presented in the graphs

(“both flow”). VEGF-A or VEGF-C were introduced into our growth factor-depleted EGM-2MV media that was incorporated into the devices. In this study, we discovered that interstitial flow in VEGF-C generates discontinuous LEC junctions, but the interstitial flow or both flow (luminal and interstitial flow) stimulates lymphatic sprouting in VEGF-A with maintaining continuous LEC junctions (Fig. 6).

In the LEC junction studies, we showed that VEGF-C loosened LEC junctions overall, and VEGF-C in the interstitial flow condition had dramatically increased cell junction discontinuities relative to all other groups (Figs. 2, 6a, b). This result indicates that interstitial flow in VEGF-C would be the best condition to simulate discontinuous LEC junctions in the initial lymphatic vessels (LVs) based on robust junction discontinuities. In nature, initial LVs mostly experience interstitial fluid pressure rather than being exposed to luminal shear stress. Interstitial flow reflects the anatomical function of initial LVs in absorbing interstitial fluid through

opening the overlapping flaps of LECs, whereas the collecting LVs that are mostly experiencing luminal flow have zipper-like junctions, which are required to maintain fluid luminally for lymph transport. Indeed, we showed that luminal flow or both flow (luminal and interstitial flow) zipped LEC junctions in VEGF-C, showing decreased junction discontinuities. This implies that lymphatic vessels prioritize responding to luminal flow over interstitial flow in their junction zipping when both flows were provided [65, 66]. Given that we used luminal shear stress of 3.5–4.5 dyne/cm² and interstitial flow of a flow rate of 1 μ m/s, further investigations remain to be performed with different levels of luminal shear stress and interstitial flow rate to determine the threshold of those flow stimuli and to know the relative contributions of each flow pattern in generating discontinuous or continuous LEC junctions.

In addition to physical factors such as luminal and interstitial flow, several biological factors have been discovered

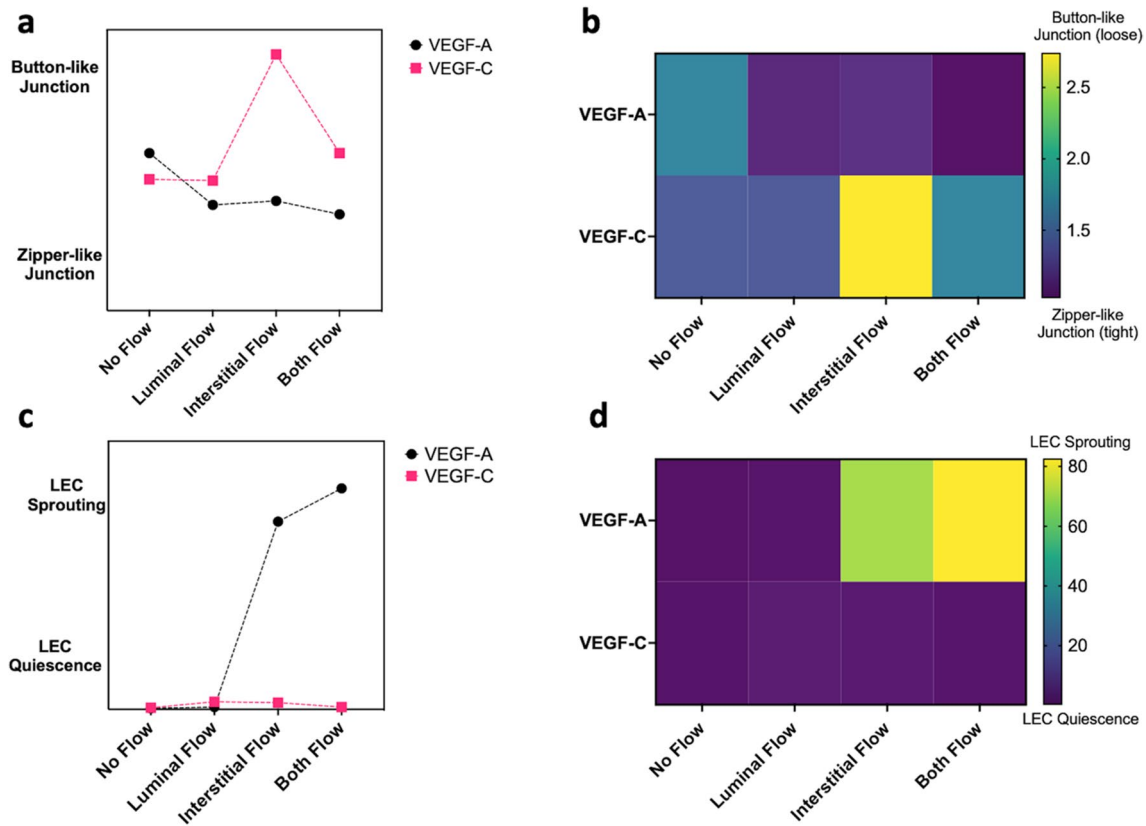


Fig. 6 Summary of junction discontinuities and sprouting with VEGF-A or VEGF-C and with different flow patterns. **a** A chart categorizing LEC junction buttoning (loose junction) or zippering (tight junction) based on flow pattern and VEGF-A or VEGF-C media. **b** Heat map categorizing LEC junction buttoning or zippering based on

flow pattern and VEGF-A or VEGF-C media. **c** A chart categorizing LEC sprouting or quiescence based on flow pattern and VEGF-A or VEGF-C media. **d** Heat map categorizing LEC sprouting or quiescence based on flow pattern and VEGF-A or VEGF-C media

that impact LEC junctions [12, 13, 18–21]. VEGF-C plays a critical role in lymphatic endothelial cell (LEC) proliferation, migration, and junction assembly [67]. Our data is consistent with current literature in that VEGF-C increased the discontinuities of LEC junctions [21], which should be a metric of lymphatic permeability. As such, our device's response to VEGF-C is consistent with other studies that report VEGF-C elevates lymphatic permeability [68]. By contrast, in the VEGF-A condition, we showed zipper-like LEC junctions in all of the flow conditions (Fig. 2), which is also consistent with the previous studies that suggest VEGF-A induces junction zippering [13, 20]. Our work adds to this collection by demonstrating that interstitial flow, modulated by VEGF-C, plays a role in inducing LEC junction buttoning.

Our research further revealed that lymphatic sprouting is induced in conditions when it receives VEGF-A and interstitial flow or both flow (interstitial and luminal flow) (Figs. 3, 6c, d). In contrast, VEGF-A with no flow or luminal flow did not trigger lymphatic sprouting; VEGF-C with all four flow conditions also did not induce any lymphatic sprouting.

These results suggest that VEGF-A and interstitial flow are the minimum requirements to promote lymphatic sprouting. These also point out that luminal flow alone could not trigger lymphatic sprouting in VEGF-A stimulation. Interestingly, it appeared that luminal flow could synergize lymphatic sprouting when both VEGF-A and interstitial flow exist, even though there was no significant difference between the VEGF-C/Interstitial Flow and VEGF-C/Both Flow groups. Related to the roles of VEGF-A in lymphatic sprouting discussed in our results, there is some evidence and research of in vitro LEC proliferation and migration by VEGF-A [69, 70]. Inhibition of VEGF-A/VEGFR2 signaling in human dermal LECs significantly reduced LEC proliferation and migration [69]. In another study, endothelial-specific molecule-1 (ESM-1), a gene that is induced by VEGF-A/VEGFR-2 activation was critical in LEC proliferation and migration [70]. However, it is also believed that VEGF-C/VEGFR3 signaling is the primary path of lymphangiogenesis [23, 67]. Nevertheless, strikingly, our VEGF-C groups did not induce lymphatic sprouting in all flow patterns. While lesser understood as a lymphangiogenic

factor, perhaps VEGF-A in our in vitro setting was only able to stimulate sprouting under the influence of interstitial flow across the 2.5 mg/mL collagen 1 hydrogel. Making endothelial sprouting with cell invasion into 3D collagen might not be a trivial process compared to other gel types such as fibrin gel or Matrigel. Also, the concentration of collagen 1 might also affect lymphatic sprouting. Different hydrogels with different concentrations and stiffnesses are to be tested in the settings to better decipher the roles of flow patterns and VEGF-A/C in lymphatic sprouting. Related to these findings, Notch signaling might provide some clues since the Notch signal has been implicated in lymphatic sprouting. It has been reported that suppression of Notch signaling synergized with VEGF-A in lymphatic sprouting [71]. This study suggested that Notch pathways induce LEC quiescence, preventing sprouting, but Notch inhibition triggers lymphatic sprouting in the presence of VEGF-A [71]. In another study, Choi et al. described that reduced Notch signaling promoted lymphatic sprouting under laminar shear flow [34]. Based on these studies, further investigations are warranted to examine Notch activities in the luminal and interstitial flow conditions in VEGF-A/C to understand whether certain flow/growth factor conditions more potently inhibit or degrade Notch and promote lymphatic sprouting.

Lastly, we showed that lymphatic sprouting under interstitial flow in VEGF-A maintained zipper junctions in engineered LVs (Fig. 2). This might be because of the VEGF-A effect on junction zipping, however, even without considering VEGF-A, this result is worth further discussing. In general, blood vessels destabilize junctions when they sprout and stabilize their junctions when they mature [72]. By contrast, lymphatic vessels in their early development, maintain zippers and later develop more buttons when they mature [13, 19]. Moreover, in adult animals, inflammation-induced lymphatic sprouting showed zipper junctions [12, 18, 19]. In this sense, our data showing zippers in sprouting LVs is consistent with the previous observations. It is necessary to further investigate how maturation processes in lymphatic and blood vessel junctions are differently regulated in lymphangiogenesis and angiogenesis at molecular levels.

Despite the intriguing findings, our study has several limitations. Given that we used human LECs in a cylindrical channel shape, future in vitro models with anatomically realistic initial lymphatic structures of blind-ended vessels need to be developed. Performing inward permeability or drainage assays would also be useful to examine the functionality of lymphatic vessels in different flow and growth factor conditions. Mechanistic understanding of the LEC junction remodeling would also be enhanced by assessing gene expressions in the engineered lymphatic vessels in different flow conditions.

In summary, we created a human lymphatic vessel-on-chip in vitro to evaluate LEC junction formation and

lymphatic sprouting in the luminal and interstitial flow, under VEGF-A or VEGF-C stimulation. We found that VEGF-C, when under interstitial flow, increases junction discontinuities that may be similar to the initial lymphatics' button-like junctions. We also discovered that VEGF-A, when under interstitial flow whether interstitial flow only or luminal and interstitial flow, induces significant lymphatic sprouting with maintaining the zipper junctions. The 3D lymphatic vessel-on-chip model may provide a unique platform to explore mechanisms of lymphatic junction morphogenesis and sprouting under different flow conditions and growth factors, which will enhance our understanding of lymphatic physiology and disease.

Supplementary Information The online version contains supplementary material available at <https://doi.org/10.1007/s12195-023-00780-0>.

Acknowledgments This work was performed in part at the Cornell NanoScale Facility (CNF), a member of the National Nanotechnology Coordinated Infrastructure (NNCI), which is supported by the National Science Foundation (Grant NNCI-2025233). We thank Dr. Young K. Hong (University of Southern California) for kindly supplying human dermal lymphatic endothelial cells (LECs).

Author Contributions ISI and EL conceived the ideas, designed the experiments, and interpreted the data. ISI and ARY conducted the experiments. RL designed and created the microfluidic chip molds and characterized the fluid profile in the chips. ISI, ARY, and YP analyzed the data. ISI and YP prepared the figures. ISI and EL wrote the manuscript. All authors have reviewed and approved the manuscript.

Funding The authors (I.S.I., A.R.Y., Y.P., R.L., and E.L.) were supported by NIH Grants (CA279560, AI168886, HL165135, and AI166772). A.R.Y. was supported by the NSF Graduate Research Fellowships Program (NSF GRFP). Y.P. was supported by the International Foundation for Ethical Research (IFER) Fellowship.

Data Availability All datasets generated for this study are included in the article. Additional data supporting this study's findings are available from the corresponding author upon reasonable request.

Declarations

Conflict of interest The authors (I.S.I., A.R.Y., Y.P., R.L., and E.L.) declare that the research was conducted in the absence of any commercial or financial relationships that could be construed as a potential conflict of interest.

Ethical Approval No animal or human studies were carried out by the authors for this article.

References

1. Aspelund, A., M. R. Robciuc, S. Karaman, T. Makinen, and K. Alitalo. Lymphatic system in cardiovascular medicine. *Circ. Res.* 118(3):515–530, 2016. <https://doi.org/10.1161/CIRCRESAHA.115.306544>.
2. Alitalo, K. The lymphatic vasculature in disease. *Nat. Med.* 17(11):1371–1380, 2011. <https://doi.org/10.1038/nm.2545>.

3. Permanyer, M., B. Bosnjak, and R. Forster. Dendritic cells, T cells and lymphatics: dialogues in migration and beyond. *Curr. Opin. Immunol.* 53:173–179, 2018. <https://doi.org/10.1016/j.coi.2018.05.004>.
4. Choe, K., J. Y. Jang, I. Park, Y. Kim, S. Ahn, D. Y. Park, Y. K. Hong, K. Alitalo, G. Y. Koh, and P. Kim. Intravital imaging of intestinal lacteals unveils lipid drainage through contractility. *J. Clin. Investig.* 125(11):4042–4052, 2015. <https://doi.org/10.1172/JCI76509>.
5. Louveau, A., B. A. Plog, S. Antila, K. Alitalo, M. Nedergaard, and J. Kipnis. Understanding the functions and relationships of the glymphatic system and meningeal lymphatics. *J. Clin. Investig.* 127(9):3210–3219, 2017. <https://doi.org/10.1172/JCI90603>.
6. Petrova, T. V., and G. Y. Koh. Biological functions of lymphatic vessels. *Science.* 2020. <https://doi.org/10.1126/science.aax4063>.
7. Oliver, G., J. Kipnis, G. J. Randolph, and N. L. Harvey. The lymphatic vasculature in the 21(st) century: novel functional roles in homeostasis and disease. *Cell.* 182(2):270–296, 2020. <https://doi.org/10.1016/j.cell.2020.06.039>.
8. Brix, B., O. Sery, A. Onorato, C. Ure, A. Roessler, and N. Goswami. Biology of lymphedema. *Biology (Basel).* 2021. <https://doi.org/10.3390/biology10040261>.
9. Schwartz, N., M. L. S. Chalasani, T. M. Li, Z. Feng, W. D. Shipman, and T. T. Lu. Lymphatic function in autoimmune diseases. *Front. Immunol.* 10:519, 2019. <https://doi.org/10.3389/fimmu.2019.00519>.
10. Mehrara, B. J., and A. K. Greene. Lymphedema and obesity: is there a link? *Plast. Reconstr. Surg.* 134(1):154e–160e, 2014. <https://doi.org/10.1097/PRS.0000000000000268>.
11. Da Mesquita, S., A. Louveau, A. Vaccari, I. Smirnov, R. C. Cornelison, K. M. Kingsmore, C. Contarino, S. Onengut-Gumuscu, E. Farber, D. Raper, et al. Functional aspects of meningeal lymphatics in ageing and Alzheimer's disease. *Nature.* 560(7717):185–191, 2018. <https://doi.org/10.1038/s41586-018-0368-8>.
12. Baluk, P., J. Fuxe, H. Hashizume, T. Romano, E. Lashnits, S. Butz, D. Vestweber, M. Corada, C. Molendini, E. Dejana, et al. Functionally specialized junctions between endothelial cells of lymphatic vessels. *J. Exp. Med.* 204(10):2349–2362, 2007. <https://doi.org/10.1084/jem.20062596>.
13. Zhang, F., G. Zarkada, S. Yi, and A. Eichmann. Lymphatic endothelial cell junctions: molecular regulation in physiology and diseases. *Front. Physiol.* 11:509, 2020. <https://doi.org/10.3389/fphys.2020.00509>.
14. Breslin, J. W., Y. Yang, J. P. Scallan, R. S. Sweat, S. P. Adderley, and W. L. Murfee. Lymphatic vessel network structure and physiology. *Compr. Physiol.* 9(1):207–299, 2018. <https://doi.org/10.1002/cphy.c180015>.
15. Ohtani, O., and Y. Ohtani. Organization and developmental aspects of lymphatic vessels. *Arch. Histol. Cytol.* 71(1):1–22, 2008. <https://doi.org/10.1679/aohc.71.1>.
16. Sweet, D. T., J. M. Jimenez, J. Chang, P. R. Hess, P. Mericko-Ishizuka, J. X. Fu, L. J. Xia, P. F. Davies, and M. L. Kahn. Lymph flow regulates collecting lymphatic vessel maturation in vivo. *J. Clin. Investig.* 125(8):2995–3007, 2015. <https://doi.org/10.1172/Jci79386>.
17. Kuan, E. L., S. Ivanov, E. A. Bridenbaugh, G. Victoria, W. Wang, E. W. Childs, A. M. Platt, C. V. Jakubzick, R. J. Mason, A. A. Gashev, et al. Collecting lymphatic vessel permeability facilitates adipose tissue inflammation and distribution of antigen to lymph node-homing adipose tissue dendritic cells. *J. Immunol.* 194(11):5200–5210, 2015. <https://doi.org/10.4049/jimmunol.1500221>.
18. Baluk, P., and D. M. McDonald. Buttons and zippers: endothelial junctions in lymphatic vessels. *Cold Spring Harb. Perspect. Med.* 2022. <https://doi.org/10.1101/cshperspect.a041178>.
19. Yao, L. C., P. Baluk, R. S. Srinivasan, G. Oliver, and D. M. McDonald. Plasticity of button-like junctions in the endothelium of airway lymphatics in development and inflammation. *Am. J. Pathol.* 180(6):2561–2575, 2012. <https://doi.org/10.1016/j.ajpath.2012.02.019>.
20. Zhang, F., G. Zarkada, J. Han, J. Li, A. Dubrac, R. Ola, G. Genet, K. Boye, P. Michon, S. E. Kunzel, et al. Lacteal junction zippering protects against diet-induced obesity. *Science.* 361(6402):599–603, 2018. <https://doi.org/10.1126/science.aap9331>.
21. Hong, S. P., M. J. Yang, H. Cho, I. Park, H. Bae, K. Choe, S. H. Suh, R. H. Adams, K. Alitalo, D. Lim, et al. Distinct fibroblast subsets regulate lacteal integrity through YAP/TAZ-induced VEGF-C in intestinal villi. *Nat. Commun.* 11(1):4102, 2020. <https://doi.org/10.1038/s41467-020-17886-y>.
22. Tammela, T., and K. Alitalo. Lymphangiogenesis: molecular mechanisms and future promise. *Cell.* 140(4):460–476, 2010. <https://doi.org/10.1016/j.cell.2010.01.045>.
23. Zheng, W., A. Aspelund, and K. Alitalo. Lymphangiogenic factors, mechanisms, and applications. *J. Clin. Investig.* 124(3):878–887, 2014. <https://doi.org/10.1172/JCI71603>.
24. Stacker, S. A., S. P. Williams, T. Karnezis, R. Shayan, S. B. Fox, and M. G. Achen. Lymphangiogenesis and lymphatic vessel remodelling in cancer. *Nat. Rev. Cancer.* 14(3):159–172, 2014. <https://doi.org/10.1038/nrc3677>.
25. Nagy, J. A., E. Vasile, D. Feng, C. Sundberg, L. F. Brown, E. J. Manseau, A. M. Dvorak, and H. F. Dvorak. VEGF-A induces angiogenesis, arteriogenesis, lymphangiogenesis, and vascular malformations. *Cold Spring Harb. Symp. Quant. Biol.* 67:227–237, 2002. <https://doi.org/10.1101/sqb.2002.67.227>.
26. Schwartz, M. A., and C. S. Chen. Cell biology. Deconstructing dimensionality. *Science.* 339(6118):402–404, 2013. <https://doi.org/10.1126/science.1233814>.
27. Baker, B. M., and C. S. Chen. Deconstructing the third dimension: how 3D culture microenvironments alter cellular cues. *J. Cell Sci.* 125(Pt 13):3015–3024, 2012. <https://doi.org/10.1242/jcs.079509>.
28. Rogic, A., F. Auger, and M. Skobe. Isolation of human skin lymphatic endothelial cells and 3D reconstruction of the lymphatic vasculature in vitro. In: *Lymphangiogenesis: Methods and Protocols*, Vol. 1846, edited by G. Oliver, and M. L. Kahn. New York: Springer, 2018, pp. 279–290. https://doi.org/10.1007/978-1-4939-8712-2_18.
29. Gong, M. M., K. M. Lugo-Cintrón, B. R. White, S. C. Kerr, P. M. Harari, and D. J. Beebe. Human organotypic lymphatic vessel model elucidates microenvironment-dependent signaling and barrier function. *Biomaterials.* 2019. <https://doi.org/10.1016/j.biomaterials.2019.119225>.
30. Kim, S., M. Chung, and N. L. Jeon. Three-dimensional biomimetic model to reconstitute sprouting lymphangiogenesis in vitro. *Biomaterials.* 78:115–128, 2016. <https://doi.org/10.1016/j.biomaterials.2015.11.019>.
31. Osaki, T., J. C. Serrano, and R. D. Kamm. Cooperative effects of vascular angiogenesis and lymphangiogenesis. *Regen. Eng. Transl. Med.* 4(3):120–132, 2018. <https://doi.org/10.1007/s40883-018-0054-2>.
32. Bruyere, F., L. Melen-Lamalle, S. Blacher, G. Roland, M. Thiry, L. Moons, F. Frankenne, P. Carmeliet, K. Alitalo, C. Libert, et al. Modeling lymphangiogenesis in a three-dimensional culture system. *Nat. Methods.* 5(5):431–437, 2008. <https://doi.org/10.1038/nmeth.1205>.
33. Kumaravel, S., C. A. Abbey, K. J. Bayless, and S. Chakraborty. The beta1-integrin plays a key role in LEC invasion in an optimized 3-D collagen matrix model. *Am. J. Physiol. Cell Physiol.* 319(6):C1045–C1058, 2020. <https://doi.org/10.1152/ajpcell.00299.2020>.
34. Choi, D., E. Park, E. Jung, Y. J. Seong, J. Yoo, E. Lee, M. Hong, S. Lee, H. Ishida, J. Burford, et al. Laminar flow downregulates

- Notch activity to promote lymphatic sprouting. *J. Clin. Investig.* 127(4):1225–1240, 2017. <https://doi.org/10.1172/JCI87442>.
35. Gibot, L., T. Galbraith, J. Bourland, A. Rogic, M. Skobe, and F. A. Auger. Tissue-engineered 3D human lymphatic microvascular network for in vitro studies of lymphangiogenesis. *Nat. Protoc.* 12(5):1077–1088, 2017. <https://doi.org/10.1038/nprot.2017.025>.
 36. Gibot, L., T. Galbraith, B. Kloos, S. Das, D. A. Lacroix, F. A. Auger, and M. Skobe. Cell-based approach for 3D reconstruction of lymphatic capillaries in vitro reveals distinct functions of HGF and VEGF-C in lymphangiogenesis. *Biomaterials.* 78:129–139, 2016. <https://doi.org/10.1016/j.biomaterials.2015.11.027>.
 37. Rogic, A., F. Auger, and M. Skobe. Isolation of human skin lymphatic endothelial cells and 3d reconstruction of the lymphatic vasculature in vitro. *Methods Mol. Biol.* 1846:279–290, 2018. https://doi.org/10.1007/978-1-4939-8712-2_18.
 38. Hong, J., A. Fristiohady, C. H. Nguyen, D. Milovanovic, N. Huttary, S. Krieger, J. Hong, S. Geleff, P. Birner, W. Jager, et al. Apigenin and luteolin attenuate the breaching of MDA-MB231 breast cancer spheroids through the lymph endothelial barrier in vitro. *Front. Pharmacol.* 9:220, 2018. <https://doi.org/10.3389/fphar.2018.00220>.
 39. Ayuso, J. M., M. M. Gong, M. C. Skala, P. M. Harari, and D. J. Beebe. Human tumor-lymphatic microfluidic model reveals differential conditioning of lymphatic vessels by breast cancer cells. *Adv. Healthc. Mater.* 9(3):e1900925, 2020. <https://doi.org/10.1002/adhm.201900925>.
 40. Henderson, A. R., I. S. Ilan, and E. Lee. A bioengineered lymphatic vessel model for studying lymphatic endothelial cell–cell junction and barrier function. *Microcirculation.* 2021. <https://doi.org/10.1111/micc.12730>.
 41. Bovay, E., A. Sabine, B. Prat-Luri, S. Kim, K. Son, A. H. Willrodt, C. Olsson, C. Halin, F. Kiefer, C. Betsholtz, et al. Multiple roles of lymphatic vessels in peripheral lymph node development. *J. Exp. Med.* 215(11):2760–2777, 2018. <https://doi.org/10.1084/jem.20180217>.
 42. Hakamivala, A., Y. Huang, Y. F. Chang, Z. Pan, A. Nair, J. T. Hsieh, and L. Tang. Development of 3D lymph node mimetic for studying prostate cancer metastasis. *Adv. Biosyst.* 3(9):e1900019, 2019. <https://doi.org/10.1002/adbi.201900019>.
 43. Shah, S. B., and A. Singh. Creating artificial lymphoid tissues to study immunity and hematological malignancies. *Curr. Opin. Hematol.* 24(4):377–383, 2017. <https://doi.org/10.1097/MOH.0000000000000356>.
 44. In, J., J. Ryu, H. Yu, D. Kang, T. Kim, and J. Kim. Microfluidic valvular chips and a numerical lymphatic vessel model for the study of lymph transport characteristics. *Lab Chip.* 21(11):2283–2293, 2021. <https://doi.org/10.1039/d1lc00022e>.
 45. Michalaki, E., V. N. Surya, G. G. Fuller, and A. R. Dunn. Perpendicular alignment of lymphatic endothelial cells in response to spatial gradients in wall shear stress. *Commun. Biol.* 3(1):57, 2020. <https://doi.org/10.1038/s42003-019-0732-8>.
 46. Choi, D., E. Park, E. Jung, B. Cha, S. Lee, J. Yu, P. M. Kim, S. Lee, Y. J. Hong, C. J. Koh, et al. Piezo1 incorporates mechanical force signals into the genetic program that governs lymphatic valve development and maintenance. *JCI Insight.* 2019. <https://doi.org/10.1172/jci.insight.125068>.
 47. Lugo-Cintrón, K. M., J. M. Ayuso, B. R. White, P. M. Harari, S. M. Ponik, D. J. Beebe, M. M. Gong, and M. Virumbrales-Munoz. Matrix density drives 3D organotypic lymphatic vessel activation in a microfluidic model of the breast tumor microenvironment. *Lab Chip.* 20(9):1586–1600, 2020. <https://doi.org/10.1039/d0lc00099j>.
 48. Frenkel, N., S. Poghosyan, C. R. Alarcon, S. B. Garcia, K. Queiroz, L. van den Bent, J. Laoukili, I. B. Rinkes, P. Vulto, O. Kranenburg, et al. Long-lived human lymphatic endothelial cells to study lymphatic biology and lymphatic vessel/tumor coculture in a 3D microfluidic model. *ACS Biomater. Sci. Eng.* 7(7):3030–3042, 2021. <https://doi.org/10.1021/acsbomaterials.0c01378>.
 49. Cao, X., R. Ashfaq, F. Cheng, S. Maharjan, J. Li, G. Ying, S. Hassan, H. Xiao, K. Yue, and Y. S. Zhang. A tumor-on-a-chip system with bioprinted blood and lymphatic vessel pair. *Adv. Funct. Mater.* 2019. <https://doi.org/10.1002/adfm.201807173>.
 50. Bourland, J., J. Fradette, and F. A. Auger. Tissue-engineered 3D melanoma model with blood and lymphatic capillaries for drug development. *Sci. Rep.* 8(1):13191, 2018. <https://doi.org/10.1038/s41598-018-31502-6>.
 51. Pisano, M., V. Triacca, K. A. Barbee, and M. A. Swartz. An in vitro model of the tumor-lymphatic microenvironment with simultaneous transendothelial and luminal flows reveals mechanisms of flow enhanced invasion. *Integr. Biol. (Camb.)* 7(5):525–533, 2015. <https://doi.org/10.1039/c5ib00085h>.
 52. Birmingham, K. G., M. J. O'Melia, S. Bordy, D. Reyes Aguilar, B. El-Reyas, G. Lesinski, and S. N. Thomas. Lymph node subcapsular sinus microenvironment-on-a-chip modeling shear flow relevant to lymphatic metastasis and immune cell homing. *iScience.* 23(11):101751, 2020. <https://doi.org/10.1016/j.isci.2020.101751>.
 53. Kraus, T., A. Lubitz, U. Schliesser, C. Giese, J. Reuschel, R. Brecht, J. Engert, and G. Winter. Evaluation of a 3D human artificial lymph node as test model for the assessment of immunogenicity of protein aggregates. *J. Pharm. Sci.* 108(7):2358–2366, 2019. <https://doi.org/10.1016/j.xphs.2019.02.011>.
 54. Hammel, J. H., S. R. Cook, M. C. Belanger, J. M. Munson, and R. R. Pompano. Modeling immunity in vitro: slices, chips, and engineered tissues. *Annu. Rev. Biomed. Eng.* 23:461–491, 2021. <https://doi.org/10.1146/annurev-bioeng-082420-124920>.
 55. Nguyen, D. T., E. Lee, S. Alimperti, R. J. Norgard, A. Wong, J. J. Lee, J. Eyckmans, B. Z. Stanger, and C. S. Chen. A biomimetic pancreatic cancer on-chip reveals endothelial ablation via ALK7 signaling. *Sci. Adv.* 5(8):eaav6789, 2019. <https://doi.org/10.1126/sciadv.aav6789>.
 56. Kwak, T. J., and E. Lee. Rapid multilayer microfabrication for modeling organotropic metastasis in breast cancer. *Biofabrication.* 2020. <https://doi.org/10.1088/1758-5090/abbd28>.
 57. Kwak, T. J., and E. Lee. In vitro modeling of solid tumor interactions with perfused blood vessels. *Sci. Rep.* 10(1):20142, 2020. <https://doi.org/10.1038/s41598-020-77180-1>.
 58. Soden, P. A., A. R. Henderson, and E. Lee. A microfluidic model of AQP4 polarization dynamics and fluid transport in the healthy and inflamed human brain: the first step towards glymphatics-on-a-chip. *Adv. Biol. (Weinh.)* 2022. <https://doi.org/10.1002/adbi.202200027>.
 59. Dixon, J. B., S. T. Greiner, A. A. Gashev, G. L. Cote, J. E. Moore, and D. C. Zawieja. Lymph flow, shear stress, and lymphocyte velocity in rat mesenteric prenodal lymphatics. *Microcirculation.* 13(7):597–610, 2006. <https://doi.org/10.1080/10739680600893909>.
 60. Moore, J. E., Jr., and C. D. Bertram. Lymphatic system flows. *Annu. Rev. Fluid Mech.* 50:459–482, 2018. <https://doi.org/10.1146/annurev-fluid-122316-045259>.
 61. Chary, S. R., and R. K. Jain. Direct measurement of interstitial convection and diffusion of albumin in normal and neoplastic tissues by fluorescence photobleaching. *Proc. Natl. Acad. Sci. U.S.A.* 86(14):5385–5389, 1989. <https://doi.org/10.1073/pnas.86.14.5385>.
 62. Wasson, E. M., K. Dubbin, and M. L. Moya. Go with the flow: modeling unique biological flows in engineered in vitro platforms. *Lab Chip.* 21(11):2095–2120, 2021. <https://doi.org/10.1039/d1lc00014d>.
 63. Schindelin, J., I. Arganda-Carreras, E. Frise, V. Kaynig, M. Longair, T. Pietzsch, S. Preibisch, C. Rueden, S. Saalfeld, B. Schmid, et al. Fiji: an open-source platform for biological-image analysis.

- Nat. Methods.* 9(7):676–682, 2012. <https://doi.org/10.1038/nmeth.2019>.
64. Xing, J., P. Yang, and L. Qingge. Robust 2D Otsu's algorithm for uneven illumination image segmentation. *Comput. Intell. Neurosci.* 2020:5047976, 2020. <https://doi.org/10.1155/2020/5047976>.
 65. Shields, J. D., M. E. Fleury, C. Yong, A. A. Tomei, G. J. Randolph, and M. A. Swartz. Autologous chemotaxis as a mechanism of tumor cell homing to lymphatics via interstitial flow and autocrine CCR7 signaling. *Cancer Cell.* 11(6):526–538, 2007. <https://doi.org/10.1016/j.ccr.2007.04.020>.
 66. Sweet, D. T., J. M. Jimenez, J. Chang, P. R. Hess, P. Mericko-Ishizuka, J. Fu, L. Xia, P. F. Davies, and M. L. Kahn. Lymph flow regulates collecting lymphatic vessel maturation in vivo. *J. Clin. Invest.* 125(8):2995–3007, 2015. <https://doi.org/10.1172/JCI79386>.
 67. Rauniyar, K., S. K. Jha, and M. Jeltsch. Biology of vascular endothelial growth factor C in the morphogenesis of lymphatic vessels. *Front. Bioeng. Biotechnol.* 6:7, 2018. <https://doi.org/10.3389/fbioe.2018.00007>.
 68. Breslin, J. W., S. Y. Yuan, and M. H. Wu. VEGF-C alters barrier function of cultured lymphatic endothelial cells through a VEGFR-3-dependent mechanism. *Lymphat. Res. Biol.* 5(2):105–113, 2007. <https://doi.org/10.1089/lrb.2007.1004>.
 69. Dellinger, M. T., and R. A. Brekken. Phosphorylation of Akt and ERK1/2 is required for VEGF-A/VEGFR2-induced proliferation and migration of lymphatic endothelium. *PLoS ONE.* 6(12):e28947, 2011. <https://doi.org/10.1371/journal.pone.0028947>.
 70. Shin, J. W., R. Huggenberger, and M. Detmar. Transcriptional profiling of VEGF-A and VEGF-C target genes in lymphatic endothelium reveals endothelial-specific molecule-1 as a novel mediator of lymphangiogenesis. *Blood.* 112(6):2318–2326, 2008. <https://doi.org/10.1182/blood-2008-05-156331>.
 71. Zheng, W., T. Tammela, M. Yamamoto, A. Anisimov, T. Holopainen, S. Kaijalainen, T. Karpanen, K. Lehti, S. Yla-Herttuala, and K. Alitalo. Notch restricts lymphatic vessel sprouting induced by vascular endothelial growth factor. *Blood.* 118(4):1154–1162, 2011. <https://doi.org/10.1182/blood-2010-11-317800>.
 72. Dejana, E. Endothelial adherens junctions: implications in the control of vascular permeability and angiogenesis. *J. Clin. Investig.* 100(11 Suppl):S7–S10, 1997.

Publisher's Note Springer Nature remains neutral with regard to jurisdictional claims in published maps and institutional affiliations.

Springer Nature or its licensor (e.g. a society or other partner) holds exclusive rights to this article under a publishing agreement with the author(s) or other rightsholder(s); author self-archiving of the accepted manuscript version of this article is solely governed by the terms of such publishing agreement and applicable law.